Bull. Chem. Soc. Jpn., ***69***, *2173—2178 (1996)*

A Simple New Method for Determining Diffusion Coefficients of Interacting Particles in Porous Silica and Gels

Shigeo Sasaki* and Hiroshi Maeda

Department of Chemistry, Faculty of Science, Kyushu University 33, Hakozaki, Higashi-ku, Fukuoka 812

(Received February 19, 1996)

A new experimental method to measure the diffusion coefficients of interacting particles in porous silica is described. The diffusion behavior of $NaNO_3$ from a porous silica sphere into a solution of NaCl was found to be very sensitive to the cross diffusion term when the concentration ratio of NaCl to $NaNO_3$ was high. The diffusion behavior of NaCl, KNO_3, and KI from the inside to the outside of the sphere was also examined. Theoretical equations to analyze the cross diffusion flows of interacting particles were derived. The cross diffusion coefficient of $NaNO_3$ and NaCl as well as the diffusion coefficients $NaNO_3$, NaCl, KNO_3, and KI in porous silica were evaluated from the present experimental results. The obtained diffusion coefficients were found to be about one third of those in solution. The diffusion behavior of $NaNO_3$, NaCl, KNO_3, and KI from spherical polyacrylamide gel was also examined for comparison.

Cross diffusion coefficients of interacting molecules are a good measure of interaction. However, due to a lack of handy methods to measure these coefficients, progress in understanding the cross diffusion coefficients has not been rapid. Only several molecular pairs such as KCl–NaCl,[1)] raffinose–urea,[2)] and dextran–albumin[3)] have been measured.

The following points should be obtained when measuring diffusion coefficients. A geometrically well-defined interface should be made between solutions of different compositions. No turbulence in the solutions during the measurements should occur. To attain these requirements, the Guoy diffusiometer[4)] has been invented. However, this apparatus cannot avoid the effect of gravity on the diffusion flow because the diffusion is designed to occur in the direction of gravity. If density inversion occurs once due to the diffusion, structured flow will also occur and the transportation of the molecules in this case cannot be diffusion.[5)]

In this respect, a porous material has some advantages. The interface between the material and the solution can be well-defined and turbulence is highly suppressed inside the material. The effect of gravity on the transportation of molecules is greatly reduced. These advantages for measuring diffusion coefficients have been demonstrated by Wall et al.[6,7)] with using porcelain plates. In their experiments, the diffusion flow behavior of salt[6)] and polymer molecules[7)] from the inside to the outside has been monitored by weighing the plates. To accurately monitor the change of weight, the initial solute concentrations should be as high as 0.1 mol dm^{-3} for the salt solution[6)] and 3% for the polymer solution.[7)] We have developed their method to be applicable to low concentration solutions and multi-component systems in order to measure cross diffusion coefficients. In the present experiments, the optical absorbance of the outer solution was monitored to observe the concentration of the solution outside the sphere. A theoretical equation for diffusion in a ternary system was derived and used to determine the cross diffusion coefficients. From the leakage behavior of $NaNO_3$ from porous silica spheres under conditions which NaCl penetrates into them, their cross diffusion coefficients were evaluated. The diffusion coefficients of $NaNO_3$, NaCl, KNO_3, and KI were also evaluated in the present experiments. The leakage behaviors of $NaNO_3$, NaCl, KNO_3, and KI from the spherical gel were also examined for comparison.

Theory

A formulation of single-component diffusion in a spherically symmetrical system is briefly described. Diffusion flow occurs in the sphere and the concentration of the solute outside the sphere, $C^{\mathrm{out}}(t)$, is assumed to always be homogeneous. At the initial time, the concentration inside the sphere is homogeneous. The concentration as a function of time and space can be derived from the following diffusion equation.

$$\frac{\partial}{\partial t}C(r,t) = D\nabla^2 C(r,t). \qquad (r \leq a) \tag{1}$$

The radial distance r from the center of the sphere is the only space variable in Eq. 1, since the present system is spherically symmetric. The solution of Eq. 1 under the following boundary conditions

$$C(r \leq a, t=0) = C_0^{\mathrm{in}} \ ; \ C(r \leq a, t=\infty) = C' \ \ (= C^{\mathrm{out}}(t=\infty)) \tag{2}$$

is easily obtained as follows

$$C(r,t) = \sum_{n=1}^{\infty} R_n \frac{\sin\left(\dfrac{n\pi}{a}r\right)}{r} \mathrm{e}^{-D\left(\frac{n\pi}{a}\right)^2 t} + C'$$
$$R_n = (-1)^{n+1}\frac{2a}{n\pi}(C_0^{\mathrm{in}} - C'). \tag{3}$$

Here a, C_0^{in}, and C' are the radius of the sphere, the concentration inside the sphere at the initial time, and the concentration at infinity time, respectively, when the concentration is uniform both inside and outside the sphere. According to the mass conservation rule, C' can be related to C_0^{out} (the initial concentration outside the sphere) as follows.

$$C' = \frac{\frac{4\pi}{3}a^3 f C_0^{\mathrm{in}} + V_0 C_0^{\mathrm{out}}}{\frac{4\pi}{3}a^3 f + V_0}, \qquad (4)$$

where V_0 is the solution volume outside the gel. Here the volume fraction of the pores in the sphere is denoted by f, which is assumed to be a constant throughout the sphere. The mass conservation rule also gives the concentration outside the sphere at any time, $C^{\mathrm{out}}(t)$, as follows.

$$\begin{aligned} C^{\mathrm{out}}(t) &= \frac{C'\left(\frac{4\pi}{3}a^3 f + V_0\right) - \int_0^a C(r,t) f 4\pi r^2 \mathrm{d}r}{V_0} \\ &= C' - \sum_{n=1}^{\infty} \frac{8fa^3}{n^2 \pi V_0}(C_0^{\mathrm{in}} - C')\mathrm{e}^{-D\left(\frac{n\pi}{a}\right)^2 t}. \end{aligned} \qquad (5)$$

A more simplified and useful expression is obtained by introducing the quantity F_1.

$$F_1(t) \equiv \frac{C^{\mathrm{out}}(t=\infty) - C^{\mathrm{out}}(t)}{C^{\mathrm{out}}(t=\infty) - C^{\mathrm{out}}(t=0)} = \frac{6}{\pi^2}\sum_{n=1}^{\infty}\frac{1}{n^2}\mathrm{e}^{-D\left(\frac{n\pi}{a}\right)^2 t}. \qquad (6)$$

For the case of cross diffusion of two solute species, the concentration of each solute can be described by the following diffusion equations.

$$\frac{\partial}{\partial t}C_1(r,t) = D_{11}\nabla^2 C_1(r,t) + D_{12}\nabla^2 C_2(r,t), \ (r \le a) \qquad (7a)$$

$$\frac{\partial}{\partial t}C_2(r,t) = D_{21}\nabla^2 C_1(r,t) + D_{22}\nabla^2 C_2(r,t). \ (r \le a) \qquad (7b)$$

In the case of an aqueous solution composed of two salts, a component of the salts is regarded as the solute species, since electrical neutrality holds in the space. The solution of Eq. 7 for spherical symmetry was newly obtained as follows. Equation 7 can be transformed to two linearly independent diffusion equations.

$$\frac{\partial}{\partial t}b_1(r,t) = \lambda_1 \nabla^2 b_1(r,t), \qquad (8a)$$

$$\frac{\partial}{\partial t}b_2(r,t) = \lambda_2 \nabla^2 b_2(r,t), \qquad (8b)$$

where

$$\lambda_1 = \frac{D_{11} + D_{22} + \sqrt{(D_{22} - D_{11})^2 + 4D_{12}D_{21}}}{2} \qquad (9a)$$

$$\lambda_2 = \frac{D_{11} + D_{22} - \sqrt{(D_{22} - D_{11})^2 + 4D_{12}D_{21}}}{2} \qquad (9b)$$

and

$$\begin{pmatrix} b_1(r,t) \\ b_2(r,t) \end{pmatrix} = \frac{1}{D_{12}(\lambda_1 - \lambda_2)}\begin{pmatrix} (\lambda_2 - D_{11}) & -D_{12} \\ (-\lambda_1 + D_{11}) & D_{12} \end{pmatrix}\begin{pmatrix} C_1(r,t) \\ C_2(r,t) \end{pmatrix}. \qquad (10)$$

According to linear algebra, $b_1(r,t)$ and $b_2(r,t)$ can be inversely transformed and $C_1(r,t)$ and $C_2(r,t)$ are given by the following relation.

$$\begin{pmatrix} C_1(r,t) \\ C_2(r,t) \end{pmatrix} = \begin{pmatrix} D_{12} & D_{12} \\ \lambda_1 - D_{11} & \lambda_2 - D_{11} \end{pmatrix}\begin{pmatrix} b_1(r,t) \\ b_2(r,t) \end{pmatrix}. \qquad (11)$$

The functions of $b_1(r,t)$ and $b_2(r,t)$ derived from Eq. 8 under the following boundary condition are solved in a manner very similar to Eq. 3.

$$C_i(r \le a,\ t=0) = C_{i0}^{\mathrm{in}};\ C_i(r \le a,\ t=\infty) = C_i' \left(= C_i^{\mathrm{out}}(t=\infty)\right) \ (i = 1,\ 2)$$

It is straightforward but tedious to derive the same type of expression as Eq. 5. The following equation for the concentration of component-1 outside the sphere, $C_1^{\mathrm{out}}(t)$, is obtained.

$$\begin{aligned} C_1^{\mathrm{out}}(t) = C_1' - \sum_n \frac{8fa^3}{n^2\pi V_0}\Bigg[&(C_{10}^{\mathrm{in}} - C_1')\mathrm{e}^{-\lambda_1\left(\frac{n\pi}{a}\right)^2 t} \\ &+ \left(\mathrm{e}^{-\lambda_2\left(\frac{n\pi}{a}\right)^2 t} - \mathrm{e}^{-\lambda_1\left(\frac{n\pi}{a}\right)^2 t}\right) \\ &\frac{(-\lambda_1 + D_{11})(C_{10}^{\mathrm{in}} - C_1') - D_{12}(C_{20}^{\mathrm{in}} - C_2')}{\lambda_1 - \lambda_2}\Bigg]. \end{aligned} \qquad (12)$$

The following relation, corresponding to Eq. 6, can be derived from Eq. 12.

$$\begin{aligned} G_1(t) &\equiv \frac{C_1^{\mathrm{out}}(t=\infty) - C_1^{\mathrm{out}}(t)}{C_1^{\mathrm{out}}(t=\infty) - C_1^{\mathrm{out}}(t=0)} \\ &= \frac{6}{\pi^2(\lambda_1 - \lambda_2)} \\ &\sum \frac{1}{n^2}\left[\left(D_{11} - \lambda_2 + D_{12}\frac{C_{20}^{\mathrm{in}} - C_2'}{C_{10}^{\mathrm{in}} - C_1'}\right)\mathrm{e}^{-\lambda_1\left(\frac{n\pi}{a}\right)^2 t}\right. \\ &\left. + \left(\lambda_1 - D_{11} - D_{12}\frac{C_{20}^{\mathrm{in}} - C_2'}{C_{10}^{\mathrm{in}} - C_1'}\right)\mathrm{e}^{-\lambda_2\left(\frac{n\pi}{a}\right)^2 t}\right]. \end{aligned} \qquad (13)$$

It should be mentioned that large values of $\frac{C_{20}^{\mathrm{in}} - C_2'}{C_{10}^{\mathrm{in}} - C_1'}$ enhance the effect of the D_{12} term on $G_1(t)$-values.

Experimental

Spherical porous silica particles were purchased from Nacalai Tesque Inc., Kyoto, Japan. According to the supplier, their pore sizes are about 10—50 μm. The radius of the silica spheres used, a, was measured with vernier calipers and was found to be 1.76 mm. The silica spheres were rinsed thoroughly with distilled water before use. Spherical poly(acrylamide)-gels were prepared according to the procedure described in the literature.[8] A small volume (ca. 100 $\mathrm{mm^3}$) of an aqueous solution of acrylamide (2 $\mathrm{mol\,dm^{-3}}$), N,N'-methylenediacrylamide (0.01 $\mathrm{mol\,dm^{-3}}$) and ammonium persulfate (0.005 $\mathrm{mol\,dm^{-3}}$) was added drop-wise into paraffin oil at 60 °C in a petri dish. The solution formed a spherical droplet on the Teflon® sheet lying at the bottom of the dish and turned into a spherical gel. The synthesized gels were rinsed thoroughly with 10^{-3} $\mathrm{mol\,dm^{-3}}$ sodium dodecyl sulfate aqueous solution and distilled water before use. The radius of the gels was estimated from the weight, W, on the basis of the relation $\frac{4\pi a^3}{3} = \frac{W}{\rho}$, where ρ is the density of the solution. No volume change of the gel was confirmed by the fact that the weight of gel after the measurement was the same as the initial value. The values of f for the silica and the gel were found to be 0.53 and 0.99, respectively, by using the relation of Eq. 4 for the measured values of a, C_0^{in}, C_0^{out}, C', and V_0. All chemicals used were of reagent grade.

The diffusion measurements were carried out as follows. The sphere was immersed into a solution of $NaNO_3$, KNO_3, KI, or NaCl of a given concentration (1×10^{-2} mol dm^{-3} for $NaNO_3$ and KNO_3, 2×10^{-3} mol dm^{-3} for KI or 1×10^{-1} mol dm^{-3} for NaCl) for more than 1 d. The sphere was then put into the optical cell shown in Fig. 1, after carefully removing the solution attached to the surface with filter paper. The sphere was suspended in the plastic net above the optical path and the solution in the cell was thoroughly stirred (about 100 rpm) to keep solute concentrations outside the sphere homogeneous. Measurement of the optical absorbance was carried out using a spectrophotometer (Ubest-50 Japan Spectroscopic Co., Ltd.) at 25.0±0.5 °C. The relative absorbance (Ab(t)−Ab(0), where Ab(t) is the absorbance at time t) was proportional to the concentration of the solute, since the observed absorbance values were within a range where a linear relation between the absorbance and the concentration held. The absorbance at 230 nm to monitor the $NaNO_3$, KNO_3, or KI concentration was recorded as a function of time. For monitoring NaCl concentrations, the absorbance at 195 nm was recorded.

Results

Typical time courses of the absorbance changes due to leakage of a single component ($NaNO_3$) from gel spheres of various radii are shown in Fig. 2. The condition of the experiment were as follows: $C_0^{\text{in}}=10^{-2}$ mol dm^{-3}, $C_0^{\text{out}}=0$ mol dm^{-3}, and $V_0=2.5$ cm^3. Values of $F_1(t)$ or $G_1(t)$ are given as $\delta\text{Ab}(t)/\delta\text{Ab}(0)$ where $\delta\text{Ab}(t)=\text{Ab}(\infty)-\text{Ab}(t)$. The values of $F_1(t)$ lie on a single curve against ta^{-2} -values as shown in Fig. 3. This indicates that Eq. 6 with $D=1.15\times10^{-9}$ m^2 s^{-1} adequately describes the leakage behavior from the gel sphere in the present study. This means that Eq. 6 can be applicable to the determination of the diffusion coefficient. The obtained D-value was found to be smaller than that in aqueous solution ($D^{\text{sol}}=1.5\times10^{-9}$ m^2 s^{-1} 9)). Small values of D were also obtained for the leakage behaviors of KNO_3, KI, and NaCl. The applicability of Eq. 6 to these leakage behaviors from porous silica spheres was examined as shown in Fig. 4. The obtained D-values are much smaller than the D^{sol}-values. However, the obtained D-values for both the porous silica and the gel were found to be proportional to those in aqueous solution as shown in Fig. 5. The proportional constants for the silica and the gel were 0.35±0.03 and 0.79±0.05, respectively. To examine the possible solute adsorption to the silica, measurements in 1 mol dm^{-3} NaCl solution were also made and the D-value of KNO_3 in the sphere was found to be 0.60×10^{-9} m^2 s^{-1}. It should be mentioned that the ratio of this value to the D-value obtained

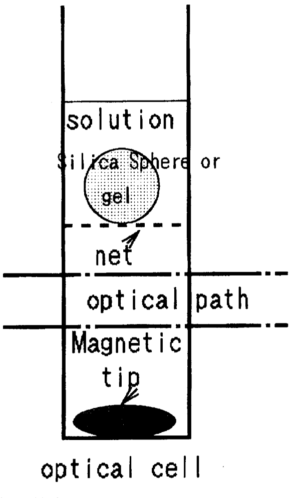

Fig. 1. Optical cell for the diffusion measurement. The cell is made of quartz. The spherical porous silica or the gel sphere is supported by the net. The magnetic tip was stirred at about 100 rpm during the measurement.

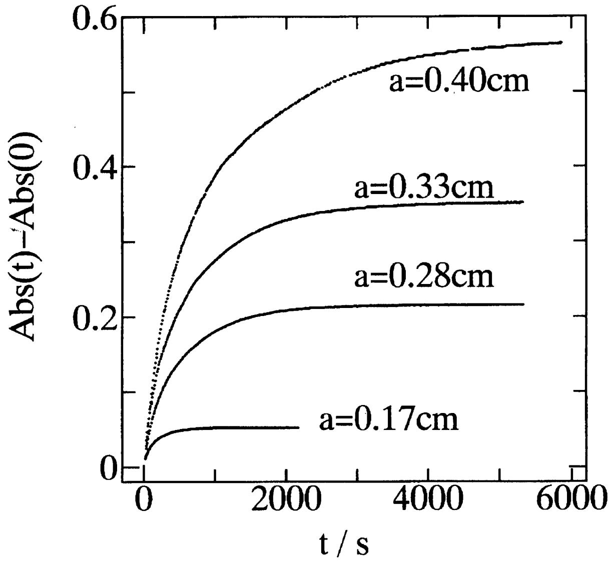

Fig. 2. Time course of the measured absorbance at $\lambda=230$ nm due to the leakage of $NaNO_3$ from the gel sphere. The concentrations of the solute at initial were $C_0{}^{\text{in}}=10^{-2}$ mol dm^{-3}, $C_0{}^{\text{out}}=0$ mol dm^{-3} and the volume outside the sphere was $V_0=2.5$ cm^3. a in the figure denotes the radius of the gel.

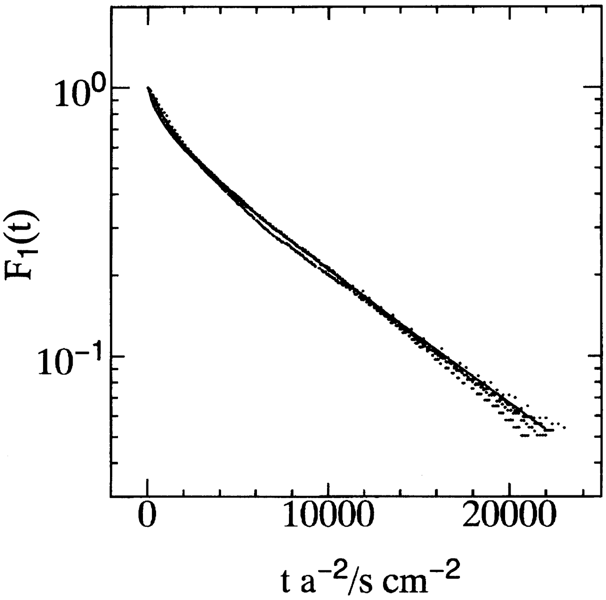

Fig. 3. Time course of the $F_1(t)$-values ($=\delta\text{Ab}(t)/\delta\text{Ab}(0)$) calculated from the data shown in Fig. 2. The $F_1(t)$-values are plotted as the solid circles against ta^{-2}-values. A solid lilne is theoretically fitted to the data with using the diffusion coefficient, $D=1.15\times10^{-9}$ m^2 s^{-1}.

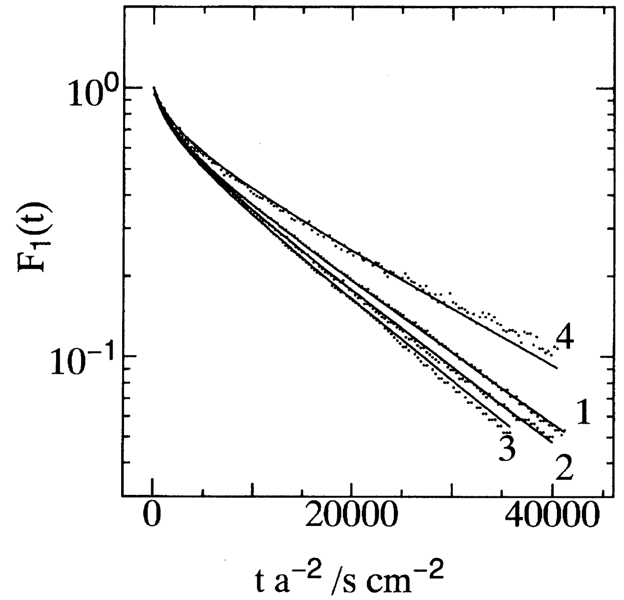

Fig. 4. Time corse of $F_1(t)$ for the diffusion of $NaNO_3$, KNO_3, KI, and NaCl in porous sphere. The concentrations of C_0^{in} are 10^{-2} mol dm^{-3} for $NaNO_3$ and KNO_3, 2×10^{-3} mol dm^{-3} for KI and 10^{-1} mol dm^{-3} for NaCl and $C_0^{\mathrm{out}}=0$ mol dm^{-3}. The $F_1(t)$-values are plotted as the solid circles against ta^{-2}-values. The solid lines: (1) $NaNO_3$; (2) KNO_3; (3) KI; (4) NaCl are theoretically fitted data with using the diffusion coefficients (10^{-9} m^2 s^{-1}): (1) $D=0.59$; (2) $D=0.66$; (3) $D=0.70$; (4) $D=0.49$.

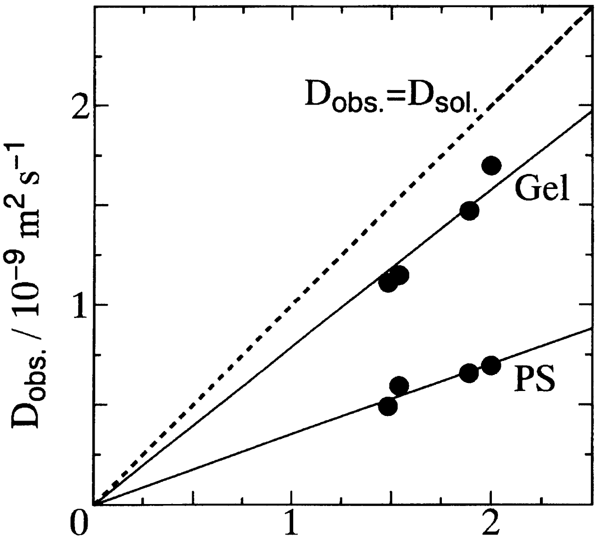

Fig. 5. Comparison of the measured diffusion coefficients of $NaNO_3$, KNO_3, KI, and NaCl in the porous sphere and the gel with their diffusion coefficients in the aqueous solution. PS and Gel, respectively, denote the porous silica and the gel. The solid and broken lines, respectively, show the relations of $D^{\mathrm{obs}}=0.35\times D^{\mathrm{sol}}$ for the porous silica, $D^{\mathrm{obs}}=0.79\times D^{\mathrm{sol}}$ for the gel and $D^{\mathrm{obs}}=D^{\mathrm{sol}}$.

for the NaCl free solution ($D=0.66\times10^{-9}$ m^2 s^{-1}) was very close to the reciprocal of the viscosity ratio (1.1) of the 1 mol dm^{-3} NaCl solution to water. This indicates the small D-values observed are not due to the effects of binding. It can be concluded that the diffusion coefficients in the porous silica or the gel are scaled down by a certain factor. When the factor is known, the porous silica or the gel can be very useful as a medium for the measurement of diffusion coefficients.

The cross diffusion experiments (measurement of $G_1(t)$) of $NaNO_3$ (component-1) and NaCl (component-2) were carried out under the following conditions: $C_{10}^{\mathrm{in}}=10^{-2}$ mol dm^{-3}; $C_{10}^{\mathrm{out}}=0$ mol dm^{-3};$C_{20}^{\mathrm{in}}=0$ mol dm^{-3}; $C_{20}^{\mathrm{out}}=10^{-1}$ mol dm^{-3}; $V_0=2.5$ cm^3. The D-values were obtained so as to minimize the difference between the experimental and the theoretical values as shown in Fig. 6. The D_{12}-values shown in Table 1 were obtained by fitting them to the data for the fixed D_{11}- and D_{22}-values (=D-values obtained in the single diffusion experiments) and the fixed value of $\frac{C_{20}^{\mathrm{in}}-C_2'}{C_{10}^{\mathrm{in}}-C_1'}=-10$. It should be noted that the theoretical $G_1(t)$-values were very insensitive to variation of the D_{21}-value. Accordingly, the obtained D_{21}-value was not accurate as shown by a large error value in Table 1. It should be mentioned that the obtained ratio of D_{12} to D_{11} (-0.019) is close to that (-0.021

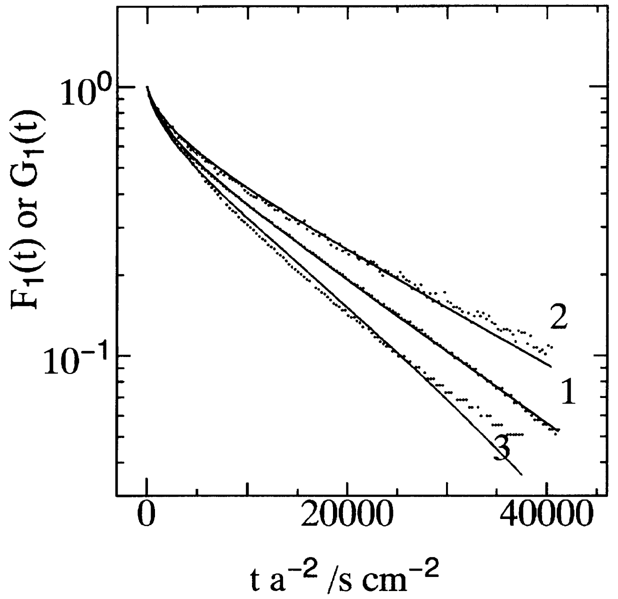

Fig. 6. Time courese of $F_1(t)$ for the diffusion of $NaNO_3$ and NaCl, and $G_1(t)$ for the diffusion of $NaNO_3$ (component 1) crossing with the counter diffusion flow of NaCl (component 2). The measured $F_1(t)$- and $G_1(t)$-values are plotted as the solid circles against ta^{-2}-values. Curves 1 and 2, respectively, are same as the curves 1 and 4 in Fig. 4, that is, the one-component diffusion $F_1(t)$ of $NaNO_3$ and NaCl. A curve 3 of the two-component diffusion $G_1(t)$ is theoretically fitted to the data with using the following diffusion coefficients (10^{-9} m^2 s^{-1}): $D_{11}=0.59$, $D_{12}=-0.012$, $D_{22}=0.49$, $D_{21}=0.0$. The concentrations of $NaNO_3$ inside the sphere and NaCl outside the sphere at the initial, respectively, are 10^{-2} mol dm^{-3} and 10^{-1} mol dm^{-3} in the case of the cross diffusion.

Table 1. Diffusion Coefficients in the Porous Silica

D_{11}[a)]	$0.59\ \pm 0.03\ \times 10^{-9}$ m^2 s^{-1}
D_{12}[b)]	$-0.011 \pm 0.003 \times 10^{-9}$ m^2 s^{-1}
D_{22}[a)]	$0.49\ \pm 0.07\ \times 10^{-9}$ m^2 s^{-1}
D_{21}[b)]	$0.0\ \pm 0.02\ \times 10^{-9}$ m^2 s^{-1}

The component-1 and -2, respectively, are NaNO$_3$ and NaCl. a) The value was obtained from the parameter fitting to the data of the one-component diffusion shown in Fig. 4. b) The values were obtained from the parameter fitting to the data of the cross diffusion shown in Fig. 6.

for $D_{12}^{\mathrm{NH}}=-0.04\times 10^{-9}$ m^2 s^{-1} and $D_{11}^{\mathrm{NH}}=1.87\times 10^{-9}$ m^2 s^{-1}) predicted by the following Nernst–Hartley equation.[1,10)]

$$D_{11}^{\mathrm{NH}} = \frac{RT}{F^2}\Lambda_{\mathrm{NO_3}}^0 \left[1 - X_{\mathrm{NO_3}}(\Lambda_{\mathrm{NO_3}}^0 - \Lambda_{\mathrm{Na}}^0)\right],$$

$$D_{12}^{\mathrm{NH}} = \frac{RT}{F^2}X_{\mathrm{NO_3}}\Lambda_{\mathrm{NO_3}}^0 \frac{\Lambda_{\mathrm{Na}}^0 - \Lambda_{\mathrm{Cl}}^0}{X_{\mathrm{NO_3}}\Lambda_{\mathrm{NO_3}}^0 + (1 - X_{\mathrm{NO_3}})\Lambda_{\mathrm{Cl}}^0 + \Lambda_{\mathrm{Na}}^0},$$

where R, T, F, Λ_{M}^0, and $X_{\mathrm{NO_3}}$ are the gas constant, temperature, Faraday constant, equivalent conductance of M-ion at infinite dilution, and concentration ratio of $\mathrm{NO_3^-}$ ion to the total anions ($X_{\mathrm{NO_3}}$ is assumed to be 0.1 in the present estimation), respectively. Considering that the Nernst–Hartley equation is valid for infinitely dilute solutions, the agreement between them can be said to be fairly good.

Discussion

The diffusion coefficients determined in the present study are given in Table 1. It is of note that the small values of the cross diffusion coefficient D_{12} were determined with reasonable accuracy by the present method. In principle, any small value of D_{12} can be obtained by setting experimental conditions in which values of the term $\left|\frac{C_{20}^{\mathrm{in}}-C_2'}{C_{10}^{\mathrm{in}}-C_1'}\right|$ in Eq. 13 are large.

When $(D_{22}-D_{11})^2 \gg D_{12}D_{21}$, Equation 13 can be approximated to

$$\begin{aligned} G_1(t) = \frac{6}{\pi^2}\sum_{n=1}^{\infty}\frac{1}{n^2}\Bigg[&\left(\frac{1}{2}\left(\frac{D_{11}-D_{22}}{|D_{22}-D_{11}|}+1\right)\right. \\ &\left.+\frac{D_{12}}{|D_{22}-D_{11}|}\frac{C_{20}^{\mathrm{in}}-C_2'}{C_{10}^{\mathrm{in}}-C_1'}\right)\mathrm{e}^{-\frac{D_{11}+D_{22}+|D_{22}-D_{11}|}{2}\left(\frac{n\pi}{a}\right)^2 t} \\ &+\left\{\frac{1}{2}\left(\frac{D_{22}-D_{11}}{|D_{22}-D_{11}|}+1\right)\right. \\ &\left.-\frac{D_{12}}{|D_{22}-D_{11}|}\frac{C_{20}^{\mathrm{in}}-C_2'}{C_{10}^{\mathrm{in}}-C_1'}\right\}\mathrm{e}^{-\frac{D_{11}+D_{22}-|D_{22}-D_{11}|}{2}\left(\frac{n\pi}{a}\right)^2 t}\Bigg] \end{aligned} \tag{14}$$

Equation 14 can be rewritten to

$$\begin{aligned} G_1(t) = \frac{6}{\pi^2}\sum_{n=1}^{\infty}\frac{1}{n^2} &\left[\left(1+s\frac{D_{12}}{|D_{22}-D_{11}|}\frac{C_{20}^{\mathrm{in}}-C_2'}{C_{10}^{\mathrm{in}}-C_1'}\right)\mathrm{e}^{-D_{11}\left(\frac{n\pi}{a}\right)^2 t}\right. \\ &\left.-s\frac{D_{12}}{|D_{22}-D_{11}|}\frac{C_{20}^{\mathrm{in}}-C_2'}{C_{10}^{\mathrm{in}}-C_1'}\mathrm{e}^{-D_{22}\left(\frac{n\pi}{a}\right)^2 t}\right] \\ s = 1 : D_{11} > D_{22};\ s &= -1 : D_{11} < D_{22} \end{aligned} \tag{14a}$$

The terms explicitly containing D_{12} in the right hand side of Eq. 14a describe the effect of the flow of component-2 on that of component-1.

It should be noted that the observed diffusion coefficients in the porous silica and the gel are 35 and 79%, respectively, of those in aqueous solution, as shown in Fig. 5. The apparent reduction of the diffusion coefficients can be interpreted as follows. In the porous silica or the polymer network molecules diffuse by passing through maze-like channels which might be narrow. In the theoretical treatment, on the other hand, the medium inside the sphere is considered to be homogeneous. That is, the random movement of the molecule in the maze is regarded as that in a homogeneous medium. The mean square displacement of the Brownian particle in the homogeneous medium, $\langle \boldsymbol{x}(t)\rangle$ is generally proportional to time t. That is,

$$\langle \boldsymbol{x}(t)^2\rangle = 6Dt \tag{15}$$

using D in Eq. 1.[11)] From the viewpoint of a coarse-grained scale, the porous material or the gel network can be regarded as homogeneous. However, from the viewpoint of a microscopic scale, the Brownian motion is under the rigid constraints of the geometrical structures of the pores and channels or the network chains. These constraints affect the random force which drives the random motion. The relation between the random force R and the Brownian motion of a particle of mass m is generally described by the following Langiven equation

$$\frac{\mathrm{d}}{\mathrm{d}t}\boldsymbol{u}(t) + \frac{\zeta}{m}\boldsymbol{u}(t) = \frac{\boldsymbol{R}(t)}{m}, \tag{16}$$

where $\boldsymbol{u}(t)$ and ζ are the velocity of the particle at t and the friction coefficient of the particle, respectively, and the correlation function of the random force is given as Eq. 17.

$$\langle \boldsymbol{R}(t_1)\cdot\boldsymbol{R}(t_2)\rangle = 6\zeta_1 kT\delta(t_1 - t_2). \tag{17}$$

Here ζ_1 is a constant. Integration of Eq. 16 gives[12)]

$$\langle \boldsymbol{u}(t)^2\rangle = 3\frac{kT}{m}\frac{\zeta_1}{\zeta} \tag{18}$$

and

$$\langle \boldsymbol{x}(t)^2\rangle = 6\frac{kT}{\zeta}\frac{\zeta_1}{\zeta}t \tag{19}$$

at $t \gg m/\zeta$. On the other hand, the equipartition law of energy gives Eq. 20 for a K_{d}-dimensional system.

$$\langle \boldsymbol{u}(t)^2\rangle = K_{\mathrm{d}}\frac{kT}{m}. \tag{20}$$

Comparing Eq. 18 with Eq. 20, we find

$$K_{\mathrm{d}} = 3\frac{\zeta_1}{\zeta}. \tag{21}$$

The following relation can then be derived from Eqs. 15 and 19.

$$D = \frac{K_{\mathrm{d}}}{3}D^{\mathrm{sol}}\ ;\ D^{\mathrm{sol}} = \frac{kT}{\zeta}. \tag{22}$$

The reduction of the dimension in the diffusion space results in the reduction of the diffusion coefficient. It should be mentional that the reduction of the apparent dimension of the diffusion space is directly related to the reduced strength of the random force as described by Eq. 17. The reduced random force results in reduced entropy force. The right hand sides in Eqs. 1 and 7 represent the effect of the entropy force or the osmotic force[13)] on the diffusion. In a multicomponent system, the diffusion of each component should be considered to be equally reduced. Therefore, the drag effect of the diffusion of the other component, the second term in the right half of Eq. 7, is reduced by the same degree as the self-diffusion term. This is suggested by the fact that the experimentally obtained value of D_{12}/D_{11} is very close to that of the theoretical prediction of the values at infinite dilution.[1,10)] For the porous silica in the present study, the experiment suggests that the apparent dimension is about 1. This might mean that molecules in the silica move along the randomly oriented and narrow tubes connecting the pores in a maze-like way.

It should be mentioned that the sign of the cross diffusion coefficient of D_{12} (1: $NaNO_3$; 2: NaCl) in the gel was found to be positive (not shown). This was opposite to the result found on the porous silica and the Nernst–Hartley prediction. The reason for this discrepancy is under investigation.

This work was partially supported by a Grant-in-Aid for Scientific Research (C) No. 08640742 from the Ministry of Education, Science, Sports and Culture.

References

1) D. G. Miller, *J. Phys. Chem.*, **71**, 616 (1967).

2) P. J. Dunlop, *J. Phys. Chem.*, **61**, 1619 (1957).

3) W. D. Comper, P. M. MacDonald, and B. N. Preston, *J. Phys. Chem.*, **88**, 6031 (1984).

4) L. J. Goesting, E. M. Hansen, G. Kegeles, and M. S. Morris, *Rev. Sci. Instrum.*, **20**, 209 (1949).

5) P. L. Vitagliano, C. D. Volpe, and V. Vitagliano, *J. Solution Chem.*, **13**, 549 (1984).

6) F. T. Wall, P. F. Grieger, and C. W. Childers, *J. Am. Chem. Soc.*, **74**, 3562 (1952).

7) F. T. Wall and C. W. Childers, *J. Am. Chem. Soc.*, **75**, 3550 (1953).

8) T. Tanaka and D. J. Fillmore, *J. Phys. Chem.*, **70**, 1214 (1979).

9) "American Institute of Physics Handbook," McGraw-Hill Book Company, Inc., New York (1957).

10) R. A. Robinson and R. H. Stokes, "Electrolyte Solutions," Butterworth Scientific Publications, London (1954), Chap. 11; W. Z. Nernst, *Phys. Chem.*, **2**, 613 (1888); G. S. Hartley, *Phys. Mag.*, **12**, 473 (1931).

11) S. Chandreasekhar, *Rev. Mod. Phys.*, **15**, 1 (1943).

12) S. Sasaki and M. Mandel, *J. Chem. Soc., Faraday Trans. 2*, **81**, 359 (1979).

13) A. Einstein, *Z. Electrochem.*, **14**, 235 (1908).